DUAL SOLUTIONS OF CONVECTION BOUNDARY LAYER FLOWS IN POROUS MEDIA, NANOFLUID AND VISCOUS FLUID

NUR FATIHAH FAUZI

UNIVERSITI SAINS MALAYSIA

2018

DUAL SOLUTIONS OF CONVECTION BOUNDARY LAYER FLOWS IN POROUS MEDIA, NANOFLUID AND VISCOUS FLUID

by

NUR FATIHAH FAUZI

Thesis submitted in fulfilment of the requirements
for the degree of
Doctor of Philosophy

May 2018

ACKNOWLEDGEMENT

In the Name of Allah, the Most Merciful, the Most Compassionate all praise be to Allah, the Lord of the worlds; and prayers and peace be upon Muhammad His servant and messenger.

First and foremost, I must acknowledge my limitless thanks to Allah, the Ever-Magnificent; the Ever-Thankful, for His help and blessings. I am absolutely certain that this work would have never progressed toward becoming truth without His guidance.

I owe a profound obligation of appreciation to our university for giving us a chance to finish this work.

I would like to express my gratitude and appreciation to my main advisor, Dr Syakila Binti Ahmad, for her guidance and all the valuable dialogs and meetings to generate new ideas, particularly during the difficult conceptual development stage. Her deep insights helped me at various stages of my research and writing of this thesis. And, I highly appreciate the efforts expended by Professor Ioan Pop, Professor John Merkin and Associate Professor Dr Lok Yian Yian.

Nevertheless, I would like to thank my fellow doctoral students for their feedback, cooperation and of course friendship. In addition, I would like to express my gratitude to the staff of School of Mathematical Sciences who gave access to the laboratory and research facilities. Without their precious support, it would not be possible to conduct this research.

I would like to take this opportunity to say warm thanks to all my beloved friends, who have been so supportive along the way of doing my thesis.

Words cannot express the feelings I have for my family for their generous support

they provided me throughout my entire life and particularly through the process of pursuing the doctorate degree. Because of their unconditional love and prayers, I have the chance to complete this thesis.

Last but not least, my deepest gratitude to those who indirectly contributed in this research, your consideration implies a great deal to me. Much thanks.

TABLE OF CONTENTS

Acknowledgement ii

Table of Contents iv

List of Tables ix

List of Figures x

List of Abbreviations xviii

List of Symbols xix

Abstrak xxv

Abstract xxvii

CHAPTER 1 – INTRODUCTION 1

1.1 Introductory Remarks 1

1.2 Basic Concepts 4

1.2.1 Heat Transfer 5

1.2.2 Boundary Layer Theory 7

1.2.3 Porous Media 11

1.2.4 Magnetohydrodynamics (MHD) 13

1.2.5 Nanofluids 14

1.2.6 Dimensionless Parameters 17

1.2.6(a) Nusselt Number 18

1.2.6(b) Prandtl Number 18

1.2.6(c) Reynolds Number 19

1.2.6(d) Schmidt Number 20

1.2.6(e) Péclet Number 21

1.2.6(f) Biot Number 22

1.2.6(g) Grashof Number 22

1.2.6(h) Lewis Number 23

1.2.6(i) Skin Friction Coefficient 23

1.2.7 Similarity Solutions 24

1.2.8 Dual Solutions of Boundary Layer Equations 26

1.2.9 Viscous Fluid 28

1.3 Significance of Fluid Flows over Spheres, Stretching/Shrinking Sheets and Flat Surfaces 28

1.4 Problem Statement 31

1.5 Objectives and Scope 32

1.6 Research Methodology 33

1.7 Thesis Outline 35

CHAPTER 2 – LITERATURE REVIEW 39

2.1 Introduction 39

2.2 Convection Flows about Spheres in Porous Media 39

2.3 Magnetohydrodynamic (MHD) Flows of Nanofluids 44

2.4 Mixed Convection Embedded in Non-Darcian Porous Media 50

2.5 Stagnation Point Flows and Heat Transfer over Shrinking Sheets 53

CHAPTER 3 – GOVERNING EQUATIONS AND NUMERICAL METHODS 60

3.1 Introduction 60

3.2 Mixed Convection Flow of Sphere through Porous Medium in Presence of Heat Generation/Absorption at Lower Stagnation Point 63

3.2.1 Dimensional Form of the Governing Equations 64

3.2.2 The Boussinesq Approximation 65

3.2.3 Non-Dimensional Form of the Governing Equations 69

3.2.4 Order of Magnitude Analysis (OMA) 72

3.3 Constant Surface Heat Flux 81

3.3.1 Nonsimilar Transformation 82

3.3.2 Numerical Method of Solution - The Keller-Box Method 85

3.3.2(a) The Finite Difference Method 86

3.3.2(b) Newton Method 89

3.3.2(c) Block Elimination Method 91

3.3.2(d) Initial Conditions 98

3.3.3 Results and Discussion 102

3.4 Constant Surface Temperature 113

3.4.1 Nonsimilar Transformation 113

3.4.2 Numerical Method of Solution - The Shooting Method 114

3.4.3 Results and Discussion 117

3.5 Conclusions 127

CHAPTER 4 – MAGNETOHYDRODYNAMICS (MHD) STAGNATION POINT FLOW OVER A STRETCHING/SHRINKING SHEET IN A NANOFLUID WITH HEAT ABSORPTION AND CONVECTIVE BOUNDARY CONDITION 130

4.1 Introduction 130

4.2 Dimensional Form of the Governing Equations 131

4.3 Non-Dimensional Form of the Governing Equations 135

4.4 Order of Magnitude Analysis 137

4.5 Nonsimilar Transformation 143

4.6 Numerical Method of Solution..... 145

4.7 Results and Discussion 147

4.8 Conclusions 173

CHAPTER 5 – MIXED CONVECTION FLOW ON A VERTICAL FLAT SURFACE WITH MELTING EFFECT IN A NON-DARCIAN POROUS MEDIUM..... 175

5.1 Introduction 175

5.2 Dimensional Form of the Governing Equations 176

5.3 Non-Dimensional Form of the Governing Equations..... 179

5.4 Order of Magnitude Analysis 180

5.5 Nonsimilar Transformation 183

5.6 Numerical Method of Solution..... 184

5.7 Results and Discussion 186

5.8 Conclusions 195

CHAPTER 6 – STAGNATION POINT FLOW AND HEAT TRANSFER OVER A NONLINEAR SHRINKING SHEET WITH SUCTION AND SLIP EFFECTS 197

6.1 Introduction 197

6.2 Dimensional Form of the Governing Equations 199

6.3 Non-Dimensional Form of the Governing Equations..... 201

6.4 Order of Magnitude Analysis 202

6.5 Nonsimilar Transformation 205

6.6 Numerical Method of Solution..... 207

6.7 Results and Discussion 209

6.7.1 Effects on Slip Parameters, A and B 209

6.7.2 Effects on Suction Parameter, S 218

6.8 Conclusions 224

CHAPTER 7 – CONCLUSION 226

7.1 Summary of Research 226

7.2 Suggestions for Future Research 231

REFERENCES 233

APPENDICES

LIST OF PUBLICATIONS

LIST OF TABLES

		Page
Table 1.1	Prandtl number of different fluids (Cengel, 2007).	19
Table 3.1	Comparison of $f''(0)$ and $-\theta(0)$ with Nazar et al. (2002a) for different values of λ when $\mathrm{Pr} = 0.7$ and $k_1 = k_3 = 0$.	105
Table 3.2	Comparison of $f''(0)$ and $-\theta(0)$ with Nazar et al. (2002b) for different values of λ when $\mathrm{Pr} = 0.7$ and $k_1 = k_3 = 0$.	121
Table 6.1	Comparison of the values of critical values χ_c with Weidman et al. (2006) for $S = -0.5$, -0.25, 0, 0.25, 0.5, $m = 0$ and $\mathrm{Pr} = 0.71$.	213
Table 6.2	Comparison of $\mathrm{Re}_x^{1/2} C_f$ with Bhattacharyya et al. (2011) for $\chi = -0.25$, -0.5, -0.615, -0.75, -1, -1.15, -1.2, -1.2465 when $A = B = S = 0$, $m = 1$ and $\mathrm{Pr} = 0.71$.	221

LIST OF FIGURES

		Page
Figure 1.1	Representation of boundary layer on a flat plate.	8
Figure 1.2	Velocity and thermal boundary layers.	10
Figure 1.3	The development of viscous and inviscid regions of flow as a result of inserting a flat plate parallel into a fluid stream of uniform velocity.	29
Figure 1.4	Flow chart of research methodology.	34
Figure 3.1	The coordinate system of mixed convection of sphere with constant surface heat flux (or constant surface temperature).	81
Figure 3.2	Flow diagram for the Keller-box method.	100
Figure 3.3	Variation of the local skin friction coefficient $f''(0)$ with the parameter λ for different values of k_1 when $\mathrm{Pr} = 3.0$ and $k_3 = 0.6$.	106
Figure 3.4	Variation of the local wall temperature θ_w with the parameter λ for different values of k_1 when $\mathrm{Pr} = 3.0$ and $k_3 = 0.6$.	106
Figure 3.5	Variation of the local skin friction coefficient $f''(0)$ with parameter λ for different values of k_1 when $\mathrm{Pr} = 3.0$ and $k_3 = -0.5$.	107
Figure 3.6	Variation of the local wall temperature θ_w with the parameter λ for different values of k_1 when $\mathrm{Pr} = 3.0$ and $k_3 = -0.5$.	107
Figure 3.7	Variation of the local skin friction coefficient $f''(0)$ with the parameter λ for different values of k_3 when $\mathrm{Pr} = 3.0$ and $k_1 = 1.0$.	108
Figure 3.8	Variation of the local wall temperature θ_w with the parameter λ for different values of k_3 when $\mathrm{Pr} = 3.0$ and $k_1 = 1.0$.	108
Figure 3.9	Variation of the local skin friction coefficient $f''(0)$ with parameter λ for different values of Pr when $k_1 = 1.0$ and $k_3 = 0.6$.	109

Figure 3.10	Variation of the local wall temperature θ_w with the parameter λ for different values of Pr when $k_1 = 1.0$ and $k_3 = 0.6$.	109
Figure 3.11	Variation of the local skin friction coefficient $f''(0)$ with the parameter λ for different values of Pr when $k_1 = 1.0$ and $k_3 = -0.5$.	110
Figure 3.12	Variation of the local wall temperature θ_w with the parameter λ for different values of Pr when $k_1 = 1.0$ and $k_3 = -0.5$.	110
Figure 3.13	Velocity profile $\frac{\partial f}{\partial \eta}$ for different values of λ when Pr $= 3.0$, $k_1 = 1.0$ and $k_3 = 0.6$.	111
Figure 3.14	Temperature profile θ for different values of λ when Pr $=$ 3.0, $k_1 = 1.0$ and $k_3 = 0.6$.	111
Figure 3.15	Velocity profile $\frac{\partial f}{\partial \eta}$ for different values of λ when Pr $= 3.0$, $k_1 = 1.0$ and $k_3 = -0.5$.	112
Figure 3.16	Temperature profile θ for different values of λ when Pr $=$ 3.0, $k_1 = 1.0$ and $k_3 = -0.5$.	112
Figure 3.17	Variation of the local skin friction coefficient $f''(0)$ with the parameter λ for different values of k_1 when Pr $= 6.8$ and $k_3 = 0.6$.	121
Figure 3.18	Variation of the local heat transfer Q_w with the parameter λ for different values of k_1 when Pr $= 6.8$ and $k_3 = 0.6$.	122
Figure 3.19	Variation of the local skin friction coefficient $f''(0)$ with the parameter λ for different values of k_1 when Pr $= 6.8$ and $k_3 = -0.5$.	122
Figure 3.20	Variation of the local heat transfer Q_w with the parameter λ for different values of k_1 when Pr $= 6.8$ and $k_3 = -0.5$.	123
Figure 3.21	Variation of the local skin friction coefficient $f''(0)$ with the parameter λ for different values of k_3 when Pr $= 6.8$ and $k_1 = 1.0$.	123
Figure 3.22	Variation of the local heat transfer Q_w with the parameter λ for different values of k_3 when Pr $= 6.8$ and $k_1 = 1.0$.	124

Figure 3.23	Variation of the local skin friction coefficient $f''(0)$ with the parameter λ for different values of Pr when $k_3 = 1.0$ and $k_1 = 0.6$.	124
Figure 3.24	Variation of the local heat transfer Q_w with the parameter λ for different values of Pr when $k_3 = 1.0$ and $k_1 = 0.6$.	125
Figure 3.25	Variation of the local skin friction coefficient $f''(0)$ with the parameter λ for different values of Pr when $k_3 = 1.0$ and $k_1 = -0.5$.	125
Figure 3.26	Variation of the local heat transfer Q_w with the parameter λ for different values of Pr when $k_3 = 1.0$ and $k_1 = -0.5$.	126
Figure 3.27	Velocity profile $\frac{\partial f}{\partial \eta}$ for different values of λ when $\mathrm{Pr} = 6.8$, $k_1 = 1.0$ and $k_3 = 0.6$.	126
Figure 3.28	Temperature profile θ for different values of λ when $\mathrm{Pr} = 6.8$, $k_1 = 1.0$ and $k_3 = 0.6$.	127
Figure 4.1	The coordinate system of magnetohydrodynamics stagnation point flow over a (a) stretching/(b) shrinking sheet in a nanofluid with heat absorption and convective boundary condition.	133
Figure 4.2	Variation of the skin friction coefficient $f''(0)$ with the parameter χ for different values of S when $\mathrm{Pr} = 1$, $G = 0.5$, $k_3 = -0.5$, $\mathrm{Bi} = 0.1$, $Nt = 0.5$, $Nb = 0.1$ and $\mathrm{Le} = 3$.	155
Figure 4.3	Variation of the local Nusselt number $\mathrm{Re}_x^{-1/2}\mathrm{Nu}$ with the parameter χ for different values of S when $\mathrm{Pr} = 1$, $G = 0.5$, $k_3 = -0.5$, $\mathrm{Bi} = 0.1$, $Nt = 0.5$, $Nb = 0.1$ and $\mathrm{Le} = 3$.	156
Figure 4.4	Variation of the local Sherwood number $\mathrm{Re}_x^{-1/2}\mathrm{Sh}$ with the parameter χ for different values of S when $\mathrm{Pr} = 1$, $G = 0.5$, $k_3 = -0.5$, $\mathrm{Bi} = 0.1$, $Nt = 0.5$, $Nb = 0.1$ and $\mathrm{Le} = 3$.	156
Figure 4.5	Variation of the skin friction coefficient $f''(0)$ with the parameter χ for different values of G when $\mathrm{Pr} = 1$, $S = 4$, $k_3 = -0.5$, $\mathrm{Bi} = 0.1$, $Nt = 0.5$, $Nb = 0.1$ and $\mathrm{Le} = 3$.	157
Figure 4.6	Variation of the local Nusselt number $\mathrm{Re}_x^{-1/2}\mathrm{Nu}$ with the parameter χ for different values of G when $\mathrm{Pr} = 1$, $S = 4$, $k_3 = -0.5$, $\mathrm{Bi} = 0.1$, $Nt = 0.5$, $Nb = 0.1$ and $\mathrm{Le} = 3$.	157

Figure 4.7 Variation of the local Sherwood number $\mathrm{Re}_x^{-1/2}\mathrm{Sh}$ with the parameter χ for different values of G when $\mathrm{Pr} = 1$, $S = 4$, $k_3 = -0.5$, $\mathrm{Bi} = 0.1$, $Nt = 0.5$, $Nb = 0.1$ and $\mathrm{Le} = 3$. 158

Figure 4.8 Variation of the local Nusselt number $\mathrm{Re}_x^{-1/2}\mathrm{Nu}$ with the parameter χ for different values of Pr when $S = 4$, $G = 0.5$, $k_3 = -0.5$, $\mathrm{Bi} = 0.1$, $Nt = 0.5$, $Nb = 0.1$ and $\mathrm{Le} = 3$. 158

Figure 4.9 Variation of the local Sherwood number $\mathrm{Re}_x^{-1/2}\mathrm{Sh}$ with the parameter χ for different values of Pr when $S = 4$, $G = 0.5$, $k_3 = -0.5$, $\mathrm{Bi} = 0.1$, $Nt = 0.5$, $Nb = 0.1$ and $\mathrm{Le} = 3$. 159

Figure 4.10 Variation of the local Nusselt number $\mathrm{Re}_x^{-1/2}\mathrm{Nu}$ with the parameter χ for different values of k_3 when $\mathrm{Pr} = 1$, $S = 4$, $G = 0.5$, $\mathrm{Bi} = 0.1$, $Nt = 0.5$, $Nb = 0.1$ and $\mathrm{Le} = 3$. 159

Figure 4.11 Variation of the local Sherwood number $\mathrm{Re}_x^{-1/2}\mathrm{Sh}$ with the parameter χ for different values of k_3 when $\mathrm{Pr} = 1$, $S = 4$, $G = 0.5$, $\mathrm{Bi} = 0.1$, $Nt = 0.5$, $Nb = 0.1$ and $\mathrm{Le} = 3$. 160

Figure 4.12 Variation of the local Nusselt number $\mathrm{Re}_x^{-1/2}\mathrm{Nu}$ with the parameter χ for different values of Bi when $\mathrm{Pr} = 1$, $S = 4$, $G = 0.5$, $k_3 = -0.5$, $Nt = 0.5$, $Nb = 0.1$ and $\mathrm{Le} = 3$. 160

Figure 4.13 Variation of the local Sherwood number $\mathrm{Re}_x^{-1/2}\mathrm{Sh}$ with the parameter χ for different values of Bi when $\mathrm{Pr} = 1$, $S = 4$, $G = 0.5$, $k_3 = -0.5$, $Nt = 0.5$, $Nb = 0.1$ and $\mathrm{Le} = 3$. 161

Figure 4.14 Variation of the local Nusselt number $\mathrm{Re}_x^{-1/2}\mathrm{Nu}$ with the parameter χ for different values of Nt when $\mathrm{Pr} = 1$, $S = 4$, $G = 0.5$, $\mathrm{Bi} = 0.1$, $k_3 = -0.5$, $Nb = 0.1$ and $\mathrm{Le} = 3$. 161

Figure 4.15 Variation of the local Sherwood number $\mathrm{Re}_x^{-1/2}\mathrm{Sh}$ with the parameter χ for different values of Nt when $\mathrm{Pr} = 1$, $S = 4$, $G = 0.5$, $\mathrm{Bi} = 0.1$, $k_3 = -0.5$, $Nb = 0.1$ and $\mathrm{Le} = 3$. 162

Figure 4.16 Variation of the local Nusselt number $\mathrm{Re}_x^{-1/2}\mathrm{Nu}$ with the parameter χ for different values of Nb when $\mathrm{Pr} = 1$, $S = 4$, $G = 0.5$, $\mathrm{Bi} = 0.1$, $k_3 = -0.5$, $Nt = 0.5$ and $\mathrm{Le} = 3$. 162

Figure 4.17 Variation of the local Sherwood number $\mathrm{Re}_x^{-1/2}\mathrm{Sh}$ with the parameter χ for different values of Nb when $\mathrm{Pr} = 1$, $S = 4$, $G = 0.5$, $\mathrm{Bi} = 0.1$, $k_3 = -0.5$, $Nt = 0.5$ and $\mathrm{Le} = 3$. 163

Figure 4.18 Variation of the local Nusselt number $\mathrm{Re}_x^{-1/2}\mathrm{Nu}$ with the parameter χ for different values of Le when $\mathrm{Pr}=1$, $S=4$, $G=0.5$, $\mathrm{Bi}=0.1$, $k_3=-0.5$, $Nb=0.1$ and $Nt=0.5$. 163

Figure 4.19 Variation of the local Sherwood number $\mathrm{Re}_x^{-1/2}\mathrm{Sh}$ with the parameter χ for different values of Le when $\mathrm{Pr}=1$, $S=4$, $G=0.5$, $\mathrm{Bi}=0.1$, $k_3=-0.5$, $Nb=0.1$ and $Nt=0.5$. 164

Figure 4.20 Velocity profile for different values of S when $\mathrm{Pr}=1$, $G=0.5$, $k_3=-0.5$, $\mathrm{Bi}=0.1$, $Nt=0.5$, $Nb=0.1$ and $\mathrm{Le}=3$. 164

Figure 4.21 Temperature profile for different values of S when $\mathrm{Pr}=1$, $G=0.5$, $k_3=-0.5$, $\mathrm{Bi}=0.1$, $Nt=0.5$, $Nb=0.1$ and $\mathrm{Le}=3$. 165

Figure 4.22 Concentration profile for different values of S when $\mathrm{Pr}=1$, $G=0.5$, $k_3=-0.5$, $\mathrm{Bi}=0.1$, $Nt=0.5$, $Nb=0.1$ and $\mathrm{Le}=3$. 165

Figure 4.23 Velocity profile for different values of G when $\mathrm{Pr}=1$, $S=4$, $k_3=-0.5$, $\mathrm{Bi}=0.1$, $Nt=0.5$, $Nb=0.1$ and $\mathrm{Le}=3$. 166

Figure 4.24 Temperature profile for different values of G when $\mathrm{Pr}=1$, $S=4$, $k_3=-0.5$, $\mathrm{Bi}=0.1$, $Nt=0.5$, $Nb=0.1$ and $\mathrm{Le}=3$. 166

Figure 4.25 Concentration profile for different values of G when $\mathrm{Pr}=1$, $S=4$, $k_3=-0.5$, $\mathrm{Bi}=0.1$, $Nt=0.5$, $Nb=0.1$ and $\mathrm{Le}=3$. 167

Figure 4.26 Temperature profile for different values of Pr when $S=4$, $G=0.5$, $k_3=-0.5$, $\mathrm{Bi}=0.1$, $Nt=0.5$, $Nb=0.1$ and $\mathrm{Le}=3$. 167

Figure 4.27 Concentration profile for different values of Pr when $S=4$, $G=0.5$, $k_3=-0.5$, $\mathrm{Bi}=0.1$, $Nt=0.5$, $Nb=0.1$ and $\mathrm{Le}=3$. 168

Figure 4.28 Temperature profile for different values of k_3 when $\mathrm{Pr}=1$, $S=4$, $G=0.5$, $\mathrm{Bi}=0.1$, $Nt=0.5$, $Nb=0.1$ and $\mathrm{Le}=3$. 168

Figure 4.29 Concentration profile for different values of k_3 when $\mathrm{Pr}=1$, $S=4$, $G=0.5$, $\mathrm{Bi}=0.1$, $Nt=0.5$, $Nb=0.1$ and $\mathrm{Le}=3$. 169

Figure 4.30 Temperature profile for different values of Bi when $\mathrm{Pr}=1$, $S=4$, $G=0.5$, $k_3=-0.5$, $Nt=0.5$, $Nb=0.1$ and $\mathrm{Le}=3$. 169

Figure 4.31 Concentration profile for different values of Bi when $\mathrm{Pr}=1$, $S=4$, $G=0.5$, $k_3=-0.5$, $Nt=0.5$, $Nb=0.1$ and $\mathrm{Le}=3$. 170

Figure 4.32 Temperature profile for different values of Nt when $\mathrm{Pr}=1$, $S=4$, $G=0.5$, $\mathrm{Bi}=0.1$, $k_3=-0.5$, $Nb=0.1$ and $\mathrm{Le}=3$. 170

Figure 4.33	Concentration profile for different values of Nt when $\mathrm{Pr} = 1$, $S = 4$, $G = 0.5$, $\mathrm{Bi} = 0.1$, $k_3 = -0.5$, $Nb = 0.1$ and $\mathrm{Le} = 3$.	171
Figure 4.34	Temperature profile for different values of Nb when $\mathrm{Pr} = 1$, $S = 4$, $G = 0.5$, $\mathrm{Bi} = 0.1$, $k_3 = -0.5$, $Nt = 0.5$ and $\mathrm{Le} = 3$.	171
Figure 4.35	Concentration profile for different values of Nb when $\mathrm{Pr} = 1$, $S = 4$, $G = 0.5$, $\mathrm{Bi} = 0.1$, $k_3 = -0.5$, $Nt = 0.5$ and $\mathrm{Le} = 3$.	172
Figure 4.36	Temperature profile for different values of Le when $\mathrm{Pr} = 1$, $S = 4$, $G = 0.5$, $\mathrm{Bi} = 0.1$, $k_3 = -0.5$, $Nb = 0.1$ and $Nt = 0.5$.	172
Figure 4.37	Concentration profile for different values of Le when $\mathrm{Pr} = 1$, $S = 4$, $G = 0.5$, $\mathrm{Bi} = 0.1$, $k_3 = -0.5$, $Nb = 0.1$ and $Nt = 0.5$.	173
Figure 5.1	The coordinate system of mixed convection flow on a vertical melting in a non-Darcian porous medium.	177
Figure 5.2	Variation of the skin friction coefficient $f''(0)$ with the mixed convection parameter λ for different values of the flow inertia coefficient γ when the melting parameter $M = 0.4$.	191
Figure 5.3	Variation of the skin friction coefficient $f''(0)$ with the mixed convection parameter λ for different values of the melting parameter M when the flow inertia coefficient $\gamma = 0.5$.	192
Figure 5.4	Variation of the local heat transfer coefficient $\theta'(0)$ with the mixed convection parameter λ for different values of the flow inertia coefficient γ when the melting parameter $M = 0.4$.	192
Figure 5.5	Variation of the local heat transfer coefficient $\theta'(0)$ with the mixed convection parameter λ for different values of the melting parameter M when the flow inertia coefficient $\gamma = 0.5$.	193
Figure 5.6	Velocity profile $f'(\eta)$ for different values of the flow inertia coefficient γ when the melting parameter $M = 0.4$ and the mixed convection parameter $\lambda = 1.3$.	193
Figure 5.7	Temperature profile $\theta(\eta)$ for different values of the flow inertia coefficient γ when the melting parameter $M = 0.4$ and the mixed convection parameter $\lambda = 1.3$.	194
Figure 5.8	Velocity profile $f'(\eta)$ for different values of the melting parameter M when the flow inertia coefficient $\gamma = 0.5$ and the mixed convection parameter $\lambda = 1.5$.	194

Figure 5.9	Temperature profile $\theta(\eta)$ for different values of the melting parameter M when the flow inertia coefficient $\gamma = 0.5$ and the mixed convection parameter $\lambda = 1.5$.	195
Figure 6.1	The coordinate system of stagnation point flow and heat transfer over a nonlinear shrinking sheet with suction and slip effects.	200
Figure 6.2	Variation of the skin friction coefficient $\mathrm{Re}_x^{1/2} C_f$ with the parameter χ for different values of A when $S = 2.5$, $B = 0.5$, $m = n = 1$ and $\mathrm{Pr} = 0.71$.	213
Figure 6.3	Variation of the local Nusselt number $\mathrm{Re}_x^{1/2}\mathrm{Nu}_x$ with the parameter χ for different values of A when $S = 2.5$, $B = 0.5$, $m = n = 1$ and $\mathrm{Pr} = 0.71$.	214
Figure 6.4	Variation of the local Nusselt number $\mathrm{Re}_x^{1/2}\mathrm{Nu}_x$ with the parameter χ for different values of B when $S = 2.5$, $A = 0.5$, $m = n = 1$ and $\mathrm{Pr} = 0.71$.	214
Figure 6.5	Variation of the local Nusselt number $\mathrm{Re}_x^{1/2}\mathrm{Nu}_x$ with the parameter χ for different values of A when $B = 0.5$, $S = 2.5$, $m = 1$, $n = 0$ and $\mathrm{Pr} = 0.71$.	215
Figure 6.6	Variation of the local Nusselt number $\mathrm{Re}_x^{1/2}\mathrm{Nu}_x$ with the parameter χ for different values of B when $A = 0.5$, $S = 2.5$, $m = 1$, $n = 0$ and $\mathrm{Pr} = 0.71$.	215
Figure 6.7	Velocity profile $f'(\eta)$ for different values of A when $S = 2.5$, $B = 0.5$, $\chi = -5.0$ and $m = n = 1$.	216
Figure 6.8	Temperature profile $\theta(\eta)$ for different values of A when $S = 2.5$, $B = 0.5$, $\chi = -5.0$ and $m = n = 1$.	216
Figure 6.9	Temperature profile $\theta(\eta)$ for different values of B when $S = 2.5$, $A = 0.5$, $\chi = -5.0$ and $m = n = 1$.	217
Figure 6.10	Temperature profile $\theta(\eta)$ for different values of A when $\lambda = -5.0$, $S = 2.5$, $B = 0.5$, $m = 1$ and $n = 0$.	217
Figure 6.11	Temperature profile $\theta(\eta)$ for different values of B when $\chi = -5.0$, $S = 2.5$, $A = 0.5$, $m = 1$ and $n = 0$.	218
Figure 6.12	Variation of the skin friction coefficient $\mathrm{Re}_x^{1/2} C_f$ with the parameter χ for different values of S when $A = B = 0.5$, $m = n = 1$ and $\mathrm{Pr} = 0.71$.	221

Figure 6.13 Variation of the local Nusselt number $\mathrm{Re}_x^{1/2}\mathrm{Nu}_x$ with the parameter χ for different values of S when $A = B = 0.5$, $m = n = 1$ and $\mathrm{Pr} = 0.71$. 222

Figure 6.14 Variation of the Nusselt number $\mathrm{Re}_x^{1/2}\mathrm{Nu}_x$ with the parameter χ for different values of S when $A = B = 0.5$, $m = 1$, $n = 0$ and $\mathrm{Pr} = 0.71$. 222

Figure 6.15 Velocity profile $f'(\eta)$ for different values of S when $\chi = -0.5$, $A = B = 0.5$, and $m = n = 1$. 223

Figure 6.16 Temperature profile $\theta(\eta)$ for different values of S when $\chi = -0.5$, $A = B = 0.5$ and $m = n = 1$. 223

Figure 6.17 Temperature profile $\theta(\eta)$ for different values of S when $\chi = -0.5$, $A = B = 0.5$, $m = 1$ and $n = 0$. 224

LIST OF ABBREVIATIONS

BVP	Boundary Value Problem
HAM	Homotopy Analysis Method
IVP	Initial Value Problem
IR	Infrared
MHD	Magnetohydrodynamics
MG	Maxwell-Garnetts
OMA	Order of Magnitude Analysis
PHAM	Predictor Homotopy Analysis Method
RK4	Fourth Order Runge-Kutta Method
UV	Ultraviolet

LIST OF SYMBOLS

a	axial distance
a_c	length of the plate
a_m	radius of sphere
a_s	constant stretching/shrinking intensity
A, B	constant slip parameters
B_0	constant magnetic field strength
Bi	Biot number
c_f	heat capacity of the liquid surface
c_s	heat capacity of the solid surface
c_p	specific heat at constant pressure
C	nanoparticle volume fraction
C_F	inertial coefficient
C_f	local skin friction factor
D	constant mass diffusivity
D_B	Brownian diffusion coefficient
D_T	thermophoretic diffusion coefficient
E	Lorenzian force
f	non-dimensional stream function
$\mathfrak{F}$	constant

g	gravitational acceleration
G	constant magnetic field parameter
Gr	Grashof number
h	convective heat transfer coefficient of the fluid
H_f	heat transfer coefficient
j_w	constant surface mass flux
J	unit vector oriented along the pore velocity vector
k_1	first-order inertial parameter of porous medium
k_2	second-order inertial parameter of porous medium
k_3	heat generation/absorption parameter
K	permeability of the porous medium
L	characteristic length
Le	Lewis number
M	non-dimensional melting temperature
$\mathrm{M}(x)$	velocity slip variable
m, n	constants
Nb	Brownian motion parameter
Nt	thermophoresis parameter
Nu	local Nusselt number
$\mathrm{N}(x)$	temperature slip variable
p	pressure shift

P	pressure
Pe	Péclet number
Pr	Prandtl number
q_w	constant surface heat flux
Q_0	heat generation/absorption constant
Q_w	local heat transfer coefficient
r	radius or radial distance
$(\rho c)_f$	effective heat capacity of the ordinary fluid
$(\rho c)_p$	effective heat capacity of nanoparticle material
R	body force term
Re	Reynolds number
S	suction/injection/constant mass flux parameter
Sc	Schmidt number
Sh	local Sherwood number
T	time
T	temperature
T_0	constant
T_f	temperature of the hot fluid
T_m	constant temperature at which the porous melts/melting temperature
T_s	solid temperature
$T_w(x)$	variable temperature

$u_e(x)$	flow external velocity/local free stream velocity
$u_w(x)$	variable velocity
u	velocity components along the x axis
U_∞	free stream velocity/far (or potential) flow velocity
U_0	tangential velocity
v_e	suction/injection parameter
v	velocity components along the y axis
$\vec{V}$	velocity vector
$\vec{V}_p$	pore velocity vector
$v_w(x)$	mass flux velocity
x, y	Cartesian coordinates along and normal to the plate, respectively

Greek Letters

α	thermal diffusivity of the fluid
α_m	thermal diffusivity of the porous emdium
β	coefficient of thermal expansion
χ	constant stretching/shrinking parameter
δ	boundary layer thickness
δ_C	diffusion boundary layer thickness
δ_T	thermal boundary layer thickness
δ_V	velocity boundary layer thickness

δ_e	energy thickness
η	independent similarity variable
γ	flow inertia coefficient
κ	thermal conductivity
Λ	latent heat of the fluid
λ	mixed convection/buoyancy parameter
μ	dynamic viscosity of the fluid
ν	kinematic viscosity
ϕ	non-dimensional concentration/volume fraction function
ψ	stream function
ρ	density of the fluid
σ	constant electric conductivity
τ_w	wall shear stress
θ	non-dimensional temperature
θ_w	local wall temperature
Υ	potential function
ε	porosity parameter

Subscripts

∞	ambient/free stream condition
w	condition at the surface

c	refer to critical value

Superscripts

$\prime$	differentiation with respect to η
$*$	non-dimensional variables

PENYELESAIAN DUAL BAGI ALIRAN LAPISAN SEMPADAN OLAKAN DALAM MEDIA BERLIANG, NANOBENDALIR DAN BENDALIR LIKAT

ABSTRAK

Penyelesaian dual bagi persamaan aliran lapisan sempadan dan perpindahan haba olakan dapat diperoleh disebabkan ketaklinear persamaan pembezaan, beza parameter geometri atau bendalir mekanik. Secara eksperimen, kewujudan penyelesaian dual atau berganda adalah sukar untuk dijangka, oleh itu pengiraan bermatematik penting untuk menyediakan struktur aliran terperinci dan untuk memerhati kejadian penyelesaian dual atau berganda. Tesis ini menerangkan kajian berangka secara terperinci pada penyelesaian dual bagi masalah lapisan sempadan olakan dengan mempertimbangkan empat masalah berbeza: (1) aliran olakan bercampur bagi sfera melalui medium berliang dalam kehadiran penjanaan/penyerapan haba pada titik genangan bawah; (2) aliran titik genangan magnetohidrodinamik (MHD) ke atas lembaran meregang/mengecut dalam nanobendalir dengan penyerapan haba dan syarat sempadan olakan; (3) aliran olakan bercampur atas permukaan datar tegak dengan kesan lebur dalam medium berliang bukan Darcian; (4) aliran titik genangan dan pemindahan haba ke atas lembaran mengecut tak linear dengan kesan sedutan dan kesan gelincir. Menggunakan penjelmaan keserupaan, persamaan-persamaan pembezaan separa tak linear dijelmakan ke dalam sistem persamaan pembezaan biasa tak linear. Persamaan pembezaan biasa tak linear terturun diselesaikan menggunakan kaedah Keller-box dan kaedah tembakan yang melibatkan kaedah Runge-Kutta bersama-sama dengan pembetulan Newton Raphson. Kaedah-kaedah berangka yang digunakan dalam kajian ini masing-masing diprogramkan dalam perisian Fortran dan Maple. Pengiraan berangka dibuat untuk parameter-parameter yang berlainan ke atas aliran bendalir dan pemindahan haba ba-

gi setiap masalah tertentu. Didapati penyelesaian dual wujud dalam masalah yang dipertimbangkan bagi media berliang, nanobendalir dan bendalir likat yang mana melibatkan sfera, lembaran meregang atau mengecut dan permukaan rata tegak. Kewujudan penyelesaian dual dipengaruhi oleh parameter-parameter yang dipertimbangkan seperti parameter inersia peringkat pertama bagi medium berliang k_1, parameter penjanaan/penyerapan haba k_3, parameter olakan campuran λ, parameter sedutan/suntikan S, parameter medan magnet malar G, nombor Prandtl Pr, nombor Biot Bi, parameter termoforesis Nt, parameter gerakan Brown Nb, nombor Lewis Le, pekali inersia aliran γ, parameter lebur M and parameter gelincir malar A/B. Bagi setiap kes yang dipertimbangkan, terdapat juga kawasan penyelesaian unik dan kawasan yang tiada penyelesaian. Keputusan menunjukkan bahawa penyelesaian cabang atas adalah stabil secara linear, manakala penyelesaian cabang bawah adalah tak stabil secara linear. Didapati bahawa penyerapan haba menghasilkan nilai pekali geseran kulit dan nilai pekali pemindahan haba setempat lebih tinggi berbanding dengan penjanaan haba bagi kes suhu permukaan malar manakala bagi kes fluks haba permukaan malar, pekali suhu dinding setempat dan pekali geseran kulit masing-masing lebih tinggi untuk penjanaan haba dan penyerapan haba. Tambahan lagi, gerakan Brown dan nombor Lewis meningkatkan kedua-dua kadar pemindahan haba dan kadar pecahan isipadu nanozarah manakala parameter termoforesis masing-masing meningkatkan dan menurunkan kadar pemindahan haba dan kadar pecahan isipadu nanozarah. Selanjutnya, diperhatikan bahawa fenomena lebur menurunkan kadar pemindahan haba dan meningkatkan pemisahan lapisan sempadan pada antara muka pepejal-cecair. Sebagai tambahan, keputusan menunjukkan bahawa gelincir halaju melambatkan pemisahan lapisan sempadan manakala gelincir suhu tidak mempengaruhi pemisahan lapisan sempadan.

DUAL SOLUTIONS OF CONVECTION BOUNDARY LAYER FLOWS IN POROUS MEDIA, NANOFLUID AND VISCOUS FLUID

ABSTRACT

The dual solutions of the boundary layer flows and convective heat transfer equations can be obtained due to the nonlinearity of the differential equations and the difference of geometric or fluid mechanical parameters. Experimentally, the existence of dual or multiple solutions seem difficult to anticipate, thus mathematical computation is essential to provide the details of flow structure and to observe occurrence of dual or multiple solutions. This thesis presents a detailed numerical study on dual solutions for convection boundary layer problems by considering four different problem: (1) mixed convection flow of sphere through porous medium in presence of heat generation/absorption at lower stagnation point; (2) magnetohydrodynamics (MHD) stagnation point flow over a stretching/shrinking sheet in a nanofluid with heat absorption and convective boundary condition; (3) mixed convection flow on a vertical flat surface with melting effect in a non-Darcian porous medium; (4) stagnation point flow and heat transfer over a nonlinear shrinking sheet with suction and slip effects. Using the similarity transformation, the nonlinear partial differential equations are transformed into a system of nonlinear ordinary differential equations. The reduced nonlinear ordinary differential equations are solved using the Keller-box method and the shooting method involves Runge-Kutta method together with Newton Raphson correction. The numerical methods used in this study are programmed in Fortran and Maple softwares, respectively. Numerical computations are carried out for different parameters on fluid flow and heat transfer for each of the specific problem on hands. It is found that dual solutions exist in the considered problems of porous media, nanofluid and viscous fluid

which involves sphere, stretching or shrinking sheet and vertical flat surface. The existences of dual solutions are influenced by the considered parameters, which include the first-order inertial parameter of porous medium k_1, the heat generation/absorption parameter k_3, the mixed convection parameter λ, the suction/injection parameter S, the constant magnetic field parameter G, the Prandtl number Pr, the Biot number Bi, the thermophoresis parameter Nt, the Brownian motion parameter Nb, the Lewis number Le, the flow inertia coefficient γ, the melting parameter M and the constant slip parameter A/B. For each of the cases studied, there are also regions for unique and no solutions. The results indicate that the upper branch solution is linearly stable, while the lower branch solution is linearly unstable. It is found that the heat absorption produces higher values of the skin friction and the local heat transfer coefficients compared to the heat generation for the case of constant surface temperature, whilst for the case of constant surface heat flux, the local wall temperature and the local skin friction coefficients are higher for the heat generation and the heat absorption, respectively. In addition, the Brownian motion and the Lewis number increase both the heat transfer and the nanoparticle volume fraction rates while the thermophoresis parameter increases and decreases the heat transfer and the nanoparticle volume fraction rates, respectively. Further, it is seen that the melting phenomenon reduces the heat transfer rate and enhances the boundary layer separation at the solid-liquid interface. In addition, results showed that the velocity slip delays the boundary layer separation whereas the temperature slip does not affect the boundary layer separation.

CHAPTER 1

INTRODUCTION

1.1 Introductory Remarks

The transfer of heat through fluid (liquid or gas) caused by molecular motion is known as convection. Besides that, convection is a process whereby the energy is transferred from a surface to a fluid flowing over it as a results of a difference between the temperature of the surface and the fluid. In general, the convection type of heat transfer is divided broadly into three basic processes. The first process is named as natural (free) convection, the second process is forced and the third process is mixed or combined forced-natural convection. The temperature differences cause density gradients in the fluid medium, and in the presence of a body force such as gravity, natural convection affects arise (Kakaç, 2012). The density change gives rise to buoyancy forces. Forced convection occurs when a fluid flow is induced by an external agent, such as a fan, a blower, the winds or the motion of the heated objects itself. Therefore, in any forced convection situation, natural convection effects are also present under the presence of gravitational body forces. In addition, the situation when the effect in both forced and natural convection act simultaneously, then the process is called mixed convection, which is also known as combined forced and natural convection. The effect is particularly marked in situations where the forced fluid flow velocity is low and/or the temperature difference is large. In mixed convection flows, the relative importance of the forced and natural convection are comparable (Pop and Ingham, 2001a).

The fluid flow through porous media with different geometry has gained momentum as well. This is due to the increasing importance in the engineering and geophysical applications such as ground water flow, drying porous solids, fuel cell membranes with electrochemistry, water purification systems, packed catalytic reactors, nuclear waste disposal and underground energy transport. Accurate description of fluid flow behaviour in the porous media is essential to the successful design and operation of projects in these areas. When one thinks about porous media, the immediate concepts that come to mind are porosity, permeability and Darcy's law. The latter is probably one of the most important tools in hydrodynamics and engineering presenting numerous applications in oil recovery, chemical engineering, nuclear safety and many other engineering field. Darcy's law depicts fluid flow behaviour in porous media. Darcy's law states that the pressure gradient is linearly proportional to the fluid velocity in the porous media. Darcy's law is an approximation in describing fluid flow in porous media in situations under a limited range of low velocities. In 1901, Forchheimer has made an attempt to correct the Darcy equation by adding a second order of the velocity term (microscopic inertial effect) and corrected the Darcy equation into the Forchheimer equation (Zeng and Grigg, 2006). Next, Brinkman (1947) added the second derivatives of the velocity (macroscopic shearing effect) to the Darcy equation, resulting in the Brinkman equation (Civan and Tiab, 1991). In most porous media, the size of the pores is very small and the change of velocity across the pore throat is negligible, thus the term "non-Darcy" is used in place of "inertial effect". Non-Darcy behaviour has significant influence on effective fracture conductivity (Holditch and Morse, 1976) and gas well productivity (Guppy et al., 1982; Martins et al., 1990). In addition, the non-Darcy behaviour is important for describing flow in porous media in situations

where high velocity occurs (Zeng and Grigg, 2006).

Although extensive research work has been devoted to heat transfer in viscous (Newtonian) fluids, today, it is possible to readily manufacture nanometer-sized particles and disperse them within a base fluid such as water. These types of suspensions have been referred to as nanofluids. Many researchers have focused their attention on nanofluids due to the possibility of increasing the heat transfer in various applications including electronic cooling. Keblinski et al. (2005) reported that nanofluids tend to have substantially higher thermal conductivity than the base fluids. Another advantages of the nanofluids over conventional solid-liquid suspensions are higher specific surface area, higher stability of the colloidal suspensions, lower pumping power required to achieve the equivalent heat transfer, reduce particle clogging compared to conventional colloids and higher level of control of the thermodynamics and transport properties by varying the particle material, concentration, size and shape (Choi, 1995; Saidur et al., 2011). The study of nanofluids has become vital for the engineering applications such as in absorption refrigeration, cooling circuits, microelectromechanical systems as well as in everyday applications, for example automotive industry.

In addition, the study of dual solutions in convective heat transfer has attract much attention because of highly nonlinear problems (Mishra and Debroy, 2005). Further, as reported by (Schlichting, 1979), the nonlinearity of the differential equations, variation of geometric or fluid mechanical parameters can lead to bifurcation in the solution and thus to dual solutions. Physically, the study on dual solutions are theoretically and practically important and an interesting subject in the area of mathematics, physics and engineering. The dual solutions in boundary layer flow and heat transfer and the

applications of the knowledge on these solutions may offer significant improvements in cost, reliability and performance of many fluid dynamics and heat transfer devices.

The present study considers the problems of dual solutions of convection boundary layer flows in porous media, nanofluid and viscous fluid under the influence of various effects such as heat generation/absorption, suction, porosity, thermophoresis, Brownian motion, melting, velocity slip and thermal slip effects and steady state prevails. Five cases of boundary condition are discussed: (1) constant surface heat flux; (2) constant surface temperature; (3) no slip; (4) slip; (5) thermal convective boundary condition. The analysis include: (1) formulation of the mathematical models to obtain the governing boundary layer flow and heat transfer equations for the new models; (2) nonsimilar boundary layer transformation; (3) numerical computation using Keller-box and shooting methods. It is worth mentioning that both methods are good and efficient in solving various convective boundary layer problems (Nazar et al., 2002b, 2002a; Hamid et al., 2011; Bhattacharyya, 2011b; Aman et al., 2011, 2013; Bhattacharyya and Vajravelu, 2012; Fauzi et al., 2012; Bachok et al., 2012a, 2012c; Wan Zaimi et al., 2013; Rohni et al., 2013, 2014; Akbar et al., 2014; Bhattacharyya et al., 2014; Abbas et al., 2015; Najib et al., 2016).

1.2 Basic Concepts

Basic concepts are the establishment for improvement of a science and to avoid conceivable misconceptions. For a good understanding of thermodynamics topics, a profound study of thermodynamics ideas is essentially vital. A system experiences a process from one equilibrium state to another with certain quantity of heat transfer

and temperature is called a science of thermodynamics. The topic of heat transfer is of fundamental important in many branches of engineering. Therefore, this thesis is concerned with a theoretical study of the dual solutions of the two-dimensional steady laminar convection boundary layer flows with heat/mass transfer over a sphere, towards a stretching/shrinking sheet and past a vertical flat surface in a porous medium, nanofluid and viscous fluid subject to different boundary conditions. The contents consist of analysis of four problems described in four separate chapters. In addition, some discussions on the significance of fluid flows over spheres, stretching/shrinking sheets and flat surfaces, the problem statement, the objectives and scope, the research methodology and the thesis outline will be presented in the last subsection.

1.2.1 Heat Transfer

Heat transfer is a thermal energy transfer between bodies or through a body which happens when there is difference in temperature between two bodies. The thermal energy transfers from a region with degree of temperature is high to a region with degree of temperature is low. For a given material and mass, the higher the temperature, the greater its thermal energy. Heat always transfers spontaneously from hot to cold body. There are three modes of heat transfer namely conduction, radiation and convection.

Conduction is a transfer of heat through a body from an area of high temperature to an area of low temperature without appreciable displacement of the particles of the body (McKetta, 1992). In solids, conduction happens through stationary fluids primarily by molecular collisions. Meanwhile, conduction in fluids happens through collisions between freely moving particles. The mechanism is identical to the electron collisions

in metals.

Radiation is a transfer of heat in the form of electromagnetic waves which uses electromagnetic radiation (photons) (Incropera and De Witt, 1990). This electromagnetic radiation can travel at the speed of light and emit by any matter which its degree of temperature is above 0 degrees Kelvin ($-273°$C). The electromagnetic spectrum classifies radiation depending on its wavelengths. The major classes of radiation from long to short wavelengths are radio waves, microwaves, infrared (IR), visible light, ultraviolet (UV), x-rays and gamma rays. For the most part, radiation with longer wavelengths can penetrate through thicker solids while radiation with shorter wavelengths contains more heat and more energetic.

Convection is a process involved when the energy is transferred from a surface to a fluid flowing over it due to temperature difference between the surface and the fluid (Incropera and De Witt, 1990). In a regular convective heat transfer, a hot surface heats the surrounding fluid, which is then diverted by fluid movement, for example, wind. By supplanting the warm fluid by a cooler fluid would draw more heat away from the surface. Thusly, the rate of heat transfer is enhanced since the heated fluid is constantly supplanted by cooler fluid.

Convection can be classified into two basic processes, either natural (or free) or forced convection. In natural convection, the flow emerges when the buoyancy forces happen because of temperature difference and acts as a driving forces. In fluid motion, the flow is caused entirely by the buoyancy force that arises due to density changes. As rule, forced convection is more proficient than natural convection because of the faster

velocity of the currents and the buoyancy has little impact on the direction of flow.

In some flows in which forced and natural (buoyancy forces) effects are both important and neither one can be neglected are termed as mixed convection. Mixed convection is relatively common in nature. In more recent applications, it occurs in rotating flow loops and in the cooling minichannels in the blades of modern gas turbines. Mixed convection effects are not always undesirable. Intentionally, in some applications, the buoyancy effect is sought in order to augment heat transfer. In situations that are predominantly forced flow, buoyancy-driven effects have four types of impact on the overall flow field (Ghiaasiaan, 2011) which are:

1. They contribute (assist, resist, or do both at different parts of the flow field) to the forced-flow velocity field.

2. They cause secondary flows. The secondary flows can enhance or reduce the heat transfer rate.

3. They affect transition from laminar to turbulent flow.

4. In turbulent flow, they can modify turbulence.

1.2.2 Boundary Layer Theory

Ludwig Prandtl $(1875-1953)$ in 1904 suggested that the viscous flows can be divided into two regions; one close to the solid boundaries and other covering the rest of the flow. Later in 1905, Ludwig Prandtl published his classic paper on what he termed the "transition layer", now known as the "boundary layer", and shaped future analysis in this field. The boundary layer is the regions close to the solid boundary where the

viscosity effects are experienced by the flow. The viscosity effect is negligible outside the boundary layer and the fluid is treated as inviscid. So, a buffer region between the wall below and the inviscid free-stream above is called boundary layer. Therefore, the Navier-Stokes equations may be simplified to such an extent that it becomes possible to tackle a large number of practical problems of great importance by using the assumption proposed by Prandtl where in certain circumstances the boundary layer thickness, δ, is much smaller than the axial distance, a. This assumption is justifiable along most of the solid surface, however, it fails near the leading edge where a is small. The stages of the formation of the boundary layer growth over a flat plate is shown in Figure 1.1. The thickness of boundary layer is defined as the distance from the wall to the point where the velocity is 99% of the free stream velocity, U_∞ and the tangential velocity at the outer edge of the boundary layer is U_0 (Ghiaasiaan, 2011).

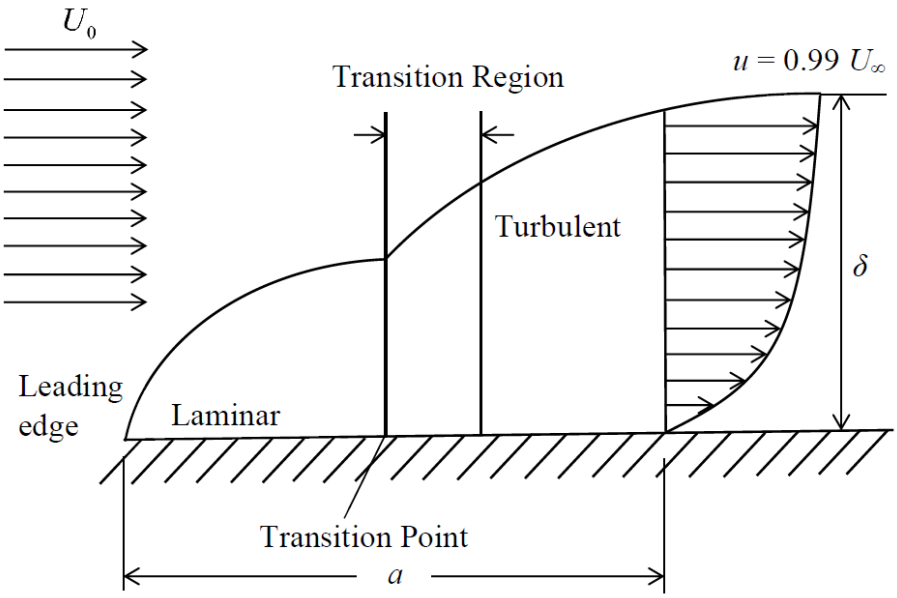

Figure 1.1: Representation of boundary layer on a flat plate.

A certain boundary layer flow is characterized by certain parameters as given below,

Boundary layer thickness (δ): It is known that no-slip conditions have to be satisfied at the solid surface which the fluid must attain the zero velocity at the wall. Subsequently, above the wall, the fluid within this layer will try to approach the free stream velocity and the effects of viscosity tends to reduce. Thus, within the fluid layers inside the small regions near to solid surface, a velocity gradient is developed. The distance from the surface to a point where the velocity equals 99% of the free stream velocity is called as boundary layer thickness. Thus, the velocity profile merges asymptotically and smoothly into the free stream. The interpretation of the boundary layer thickness is basically and generally explained by the definition of velocity boundary layer thickness.

The boundary layer can be divided into two basic types as shown in Figure 1.2 for a simple flow configuration over a flat surface. Interaction between fluid and the surface of the plate will produce a region in the fluid where the y-component velocity u rises from zero at the surface (no slip condition) to an asymptotic value equals to U_∞. This region is known as the **velocity boundary layer** where δ_V is the velocity boundary layer thickness. This layer is characterized by the velocity gradient and the shear stress. On the other hand, the existing of temperature difference between the fluid and the surface will form a region in the fluid where its temperature changing from the surface value T_s at $y = 0$ to T_∞ at the outer flow. This region is called the **thermal boundary layer** (Incropera and Dewitt, 1996) where its thickness is represented by δ_T. This thermal boundary layer is characterized by the temperature gradient and the heat transfer.

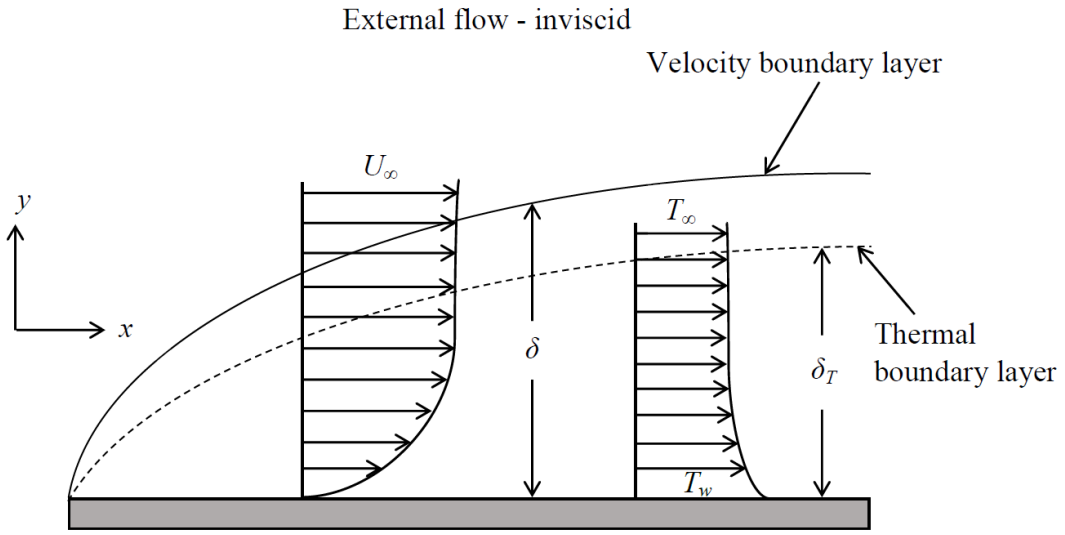

Figure 1.2: Velocity and thermal boundary layers.

The boundary layer concept is a very important tool and allows for simplifications of the analysis of virtually all transport process in two important ways (Ghiaasiaan, 2011); First, it limits the domain in the flow field where the viscous and other effects of the wall must be included in the conservation equations. Seconds, it shows that, within the boundary layer, the conservation equations can be simplified by eliminating certain terms in those equations. The most important reason is that the boundary layer equations are parabolic in nature while the full Navier-Stokes equations (developed by Navier in 1823, and subsequently by Cauchy, Poisson, Saint-Venant and in 1842 Stokes) are nonlinear and elliptical in nature, which are of considerable complexity. Hence parabolic partial differential equations can be solved much easily. However, the boundary layer equations are available only up to the separation point and beyond this point, the full Navier-Stokes equations have to be solved with much complexity. Detailed depiction of boundary layer flows can be found in the book by Schlichting and Gersten (2001). Further, in Chapter 3 of this thesis the discussions on scale (order of magnitude) analysis of boundary layer approximations are considered.

1.2.3 Porous Media

The fluid flow through porous media is important due to its practical application such as in fiber and granular insulations, winding structures for high-power density electric machines and the cores of nuclear reactors, food processing and storage, thermal insulation of buildings, geophysical systems, electro-chemistry, metallurgy, the design of pebble bed nuclear reactors, underground disposal of nuclear or non-nuclear waste, cooling system of electronic devices and many others (Nield and Bejan, 2006; Vafai, 2010; Vadasz, 2008). Flow and transport in porous media involve complex interactions between a solid matrix permeated by an interconnected of voids (pores) and a moving fluid (liquid or gas). The basic law governing the flow of fluids through porous media is known as Darcy's law and is equivalent to Ohm's law in flow of electric current. These flow occurs at very small Reynolds number $(\ll 1)$. It states that the flow rate is a function of fluid pressure, flow area and elevation (Bar-Meir, 2009). Darcy's law is an empirical law that is postulated in 1856 by engineer Henry Darcy as a results on the basis of his experimental studies on vertical water filtration through sand beds. Darcy's law applies only to the cases where the flow through pores of a porous medium can be modeled as Stokes flow. The law forms a basis for modeling fluid transport in porous media. In applications where fluid velocities are low, Darcy's law well describes the fluid transport in porous media but where the fluid velocities are high, the fluid transport predicted by Darcy's law usually departs from measurements considerably. Darcy's law only applies under certain conditions, in situations in which it does not hold inertia forces are dominant. Under the conditions where the inertia forces are dominant, then, the fluid flow is described as non-Darcy (El-Amin et al., 2008). Flow through porous media is useful to reservoir engineers who are interested in recovery

of oil or gas. Examples of fluid flow in porous media include the flow of water in aquifers, fluid flow in packed beds, irrigation problems, heat storage in beds and biological systems (Khalid et al., 2015). Many studies have been performed on the fluid flow in porous media, these contain the work of Lok et al. (2013) which deliberated the mixed convection boundary layer flow embedded in a fluid-saturated porous medium on one face of a semi-infinite vertical surface. Khalili et al. (2014) has studied the development of the unsteady two-dimensional boundary layer flow and heat transfer of a viscous nanofluid in the region of the stagnation point on a stretching/shrinking sheet in a porous medium. Recently, Kumar and Sood (2016) have investigated the unsteady magnetohydrodynamic flow in a porous medium.

Fluid flow through porous media can be solved with the help of boundary layer theory developed by Prandtl. Boundary layer theory has been proven to be of fundamental importance in Newtonian (non-porous) fluid since the concept of boundary layer can be used to simplify the Navier-Stokes equations to such an extent that it becomes possible to tackle. Wooding (1963) attempted to solve equations which govern the fluid flow and heat transfer in porous media using the boundary layer assumptions (Pop and Ingham, 2001a). Several models are proposed in order to explain the mathematical and physical aspects associated with convective boundary layers in porous media. Among these, the Darcy and a series of its modifications gained much acceptance and boundary layer assumptions are successfully applied to these models and much work over the last decades has been done on them for a large variety of body geometries and surface temperature distributions (Pop and Ingham, 2001a).

For the problems in porous media throughout this thesis, the following assumptions (Pop and Ingham, 2001a) are considered:

1. At adequately large velocities, the fluid and porous medium are not in local thermal equilibrium, i.e. the temperature T_s and T_f in the solid and fluid phases, respectively, are not indistinguishably the same.

2. The porous medium is isotropic (identical in all directions or invariant with respect to direction).

3. Viscous dissipation, radiative effects and the work done by pressure changes are negligible.

4. The Boussinesq approximation is valid.

1.2.4 Magnetohydrodynamics (MHD)

Magnetohydrodynamics or MHD is the study of fluid flow in electrically conducting fluids with magnetic properties that affect fluid flow. When magnetic field is incident in an electrically conducting fluid, a current is induced. The magnetic fields associated with the currents modify the magnetic field which makes them. Magnetic fields can have some unexpected effects on fluid flow. They can accelerate or decelerate a flow and can also induce motion in fluid. In other words, the fluid flow modifies the electromagnetic state of the system. Then again, the flow of electric current across a magnetic field is associated with a body force, the so-called Lorentz force, which influences the fluid flow. The application of a magnetic field results in controlling the momentum and heat transfer in fluid flow (Wooding, 2013).

As of late, MHD is applied to the issue of fusion power, where the application is the creation and containment of hot plasmas by electromagnetic forces since material walls would be wrecked. However, the original application of MHD in geophysical and astrophysical are still very important. The principal geophysical issue is planetary magnetism created by the currents deep in the planet while the solar structure particularly in the outer layers, interstellar magnetic fields and the solar wind bathing the earth and other planets are incorporated as the astrophysical problems. Engineers employ MHD principle in their design of heat exchangers, in creating novel power generating systems, in space vehicle propulsion, braking, pumps and flow meters, thermal protection, control and re-entry.

There are several studies that investigated MHD fluid flow; these include the work of Adeniyan and Adigun (2013) who investigated the effects of convective plane flow with convective boundary conditions in the existence of a uniform magnetic field. Abbasbandy et al. (2014) and Prakash and Muthtamilselvan (2014) have examined the effect of MHD on micropolar fluid. Later, Farooq et al. (2016) considered MHD flow of a viscoelastic nanofluid towards a stretching surface with nonlinear radiative effects.

1.2.5 Nanofluids

Nanomaterials in nanotechnology are the materials produce and process with average crystallite sizes below 100nm. Consequently, the nanotechnology provides a new area of research interest. In general, there are four types of nanomaterials such as composites, dendrimers, metal-based nanomaterials and carbon-based nanomaterials. Hence, when these nanoparticles are suspended in conventional fluids (liquid base

fluid) like water, oil, ethylene glycol, the obtained solutions are called "nanofluids". The nanolayer works as a thermal bridge between the liquid base fluid and the solid nanoparticles. Therefore, a nanofluid consists of the liquid, the nanolayers and the solid nanoparticles. The thermo-physical properties such as viscosity, thermal diffusivity, thermal conductivity and convective heat transfer coefficient are enhanced by the presence of nanofluids. Due to properties of nanofluid such as the volumetric fraction of nanoparticles, shape and size of the nanomaterials, it can be widely used for various applications of heat transfer in engineering including automotive and air conditioning cooling, improving diesel generator efficiency, cooling of transformer oil, solar and power plant cooling, in nuclear reactor for defense and space. Although the use of nanofluids will improve the overall properties and heat transfer characteristics of base fluid even then the development and applications of nanofluids may be limited by several factors due to use of very small size solid particles with very small concentration.

Nanofluids possess the following advantages as compared to conventional fluids which makes them suitable for various applications involving heat exchange:

1. Absorption of solar energy will be maximized with change of the size, shape, material and volume fraction of the nanoparticles.

2. The suspended nanoparticles increase the surface area and heat capacity of the fluid due to the very small particle size.

3. The suspended nanoparticles enhance the thermal conductivity which results improvement in efficiency of heat transfer systems (Adeniyan and Adigun, 2010).

4. Heating with the fluid volume, transferring heat to small area of fluid and allowing the peak temperature to be located away from surfaces losing heat to the environment.

5. The mixing fluctuation and turbulence of the fluid intensified.

6. The dispersion of nanoparticle flattens the transverse temperature gradient of the fluid.

7. To make suitable for different applications, properties of fluid can be changed varying concentration of nanoparticles.

Maxwell (1873) has been the first to explain that the addition of particles to a base fluid created a suspension-mix that could result in enhancing effective thermal conductivity due to the change in the combined bulk property of the base fluid and the particle. Pfautsch (2008) published an article on forced convection in nanofluids over a flat plate. Her work analyzed the characteristics, flow development and heat transfer coefficient of nanofluids under laminar forced convection over a flat plate. She concluded that varying the nanoparticle volume fraction distribution showed that it is important for the nanoparticle to stay evenly suspended throughout the flow in order to be appreciable enhancements in the heat transfer coefficient. Nanofluids have a substantially larger thermal conductivity compared to that of the common base fluids (Choi, 1995).

Among the researchers who proposed the models of nanofluid are Khanafer et al. (2003), Buongiorno (2006), Tiwari and Das (2007), Nield and Kuznetsov (2009) and Kuznetsov and Nield (2010). However, in this study, the interest is to analyze the effects of the suspended particles, Brownian motion, thermophoresis and diffusiophore-

sis. In that case, the model proposed by Buongiorno (2006) is being considered. A wide variety of fine-scale particles displays an irregular motion on a random path when suspended in a base fluid, which is known as the Brownian motion. The Brownian motion is first observed by Robert Brown in 1826 (Nelson, 1967) and is first described analytically by Einstein (1905) to determine the size of molecules. Mobile particles suspended in a liquid are subject to a force under the effect of a temperature gradient, directed in the opposite direction of the temperature gradient. This force, which is equivalent to Soret effect, is called thermophoretic force and is the result of differences in momentum and energy transferred to the particles by bombardment of higher energy molecules on the higher temperature side (Wang et al., 2012). The Soret effect occurs when the small light molecules and large heavy molecules separate under a temperature gradient. Usually this effect is important when more than one chemical species are present under a very large temperature gradient such as cardiovascular disease problems and chemical reactors. This effect is found when solving the species mass fraction equations.

1.2.6 Dimensionless Parameters

Dimensionless parameters are of key importance in parametric analysis of engineering problems. They are also useful in understanding the similarity among problems belonging to the same broad class. The dimensionless parameters that will be described in the next nine subsections are the parameters used in this thesis.

1.2.6(a) Nusselt Number

Nusselt number is a dimensionless number, named after Wilhelm Nusselt, defined as (Incropera and Dewitt, 1996; Cengel, 2007)

$$\mathrm{Nu}_L = \frac{\text{convective heat transfer}}{\text{conductive heat transfer}} = \frac{hL}{\kappa} = \frac{h\Delta T}{\kappa \Delta T/L},$$

where h is the convective heat transfer coefficient of the fluid, κ is the thermal conductivity of the fluid, L is the characteristic length and ΔT is the temperature difference. The Nusselt number represents the enhancement of heat transfer through a fluid layer as a result of convection relative to conduction across the same fluid. The larger the Nusselt number, the more effective the convection. A Nusselt number of 1 for a fluid layer represents heat transfer across the layer by pure conduction (Cengel, 2007).

Selection of the characteristic length should be in the direction of growth (or thickness) of the boundary layer, for example the diameter of a sphere, the length of a vertical plate undergoing natural convection, or the outer diameter of a cylinder in cross flow. Whereas, for complex shapes, the length may be defined as the volume of the fluid body divided by the surface area.

For engineering purposes, the thermal conductivity of the fluid is calculated as the mean-average of the bulk fluid temperature T_∞ and wall surface temperature T_w.

1.2.6(b) Prandtl Number

The Prandtl number Pr is a dimensionless number defined as the ratio of momentum diffusivity (kinematic viscosity) to thermal diffusivity (Incropera and Dewitt, 1996;

Cengel, 2007). It is named after the German physicist Ludwig Prandtl, and this number describes the relative thickness of the velocity and the thermal boundary layers. The Prandtl number can be written as

$$\mathrm{Pr} = \frac{\text{viscous diffusion rate}}{\text{thermal diffusion rate}} = \frac{\nu}{\alpha} = \frac{\mu\, c_p}{\kappa},$$

where $\nu = \dfrac{\mu}{\rho}$ is the kinematic viscosity of the fluid and $\alpha = \dfrac{\kappa}{\rho\, c_p}$ is the thermal diffusivity due to heat conduction. Table 1.1 (Cengel, 2007) shows that the Prandtl number of fluids range from less than 0.01 for liquid metals to more than 100000 for heavy oils. The Prandtl number of gases are about 1, which indicates that both heat and momentum dissipate through the fluid at about the same rate. In liquid metals ($\mathrm{Pr} \ll 1$), the heat diffuses very quickly and vice versa in oils ($\mathrm{Pr} \gg 1$). As a result, the thermal boundary layer is much thicker for liquid metals and the velocity boundary layer is much thinner for oils.

Table 1.1: Prandtl number of different fluids (Cengel, 2007).

Fluids	Pr
Liquid metals	0.004 – 0.030
Gases	0.7 – 1.0
Water	1.7 – 13.7
Light organic fluids	5 – 50
Oils	50 – 100000
Glycerin	2000 – 100000

1.2.6(c) Reynolds Number

The most important number parameter of the dynamics of viscous fluid is Reynolds number. The Reynolds number is the ratio of inertial forces to viscous forces and

defined as (Incropera and Dewitt, 1996; Cengel, 2007)

$$\mathrm{Re} = \frac{\text{inertia forces}}{\text{viscous forces}} = \frac{\rho V L}{\mu} = \frac{V L}{\nu},$$

where V is the upstream velocity (equivalent to the free stream velocity for a flat plate), L is the characteristic length of the geometry, μ is the dynamic viscosity of the fluid, ν is the kinematic viscosity and ρ is the density of the fluid.

Note that multiplying the Reynolds number by $\frac{\rho V^2 L^2}{\mu V L}$ yields $\frac{\rho V L}{\rho V L}$, which is the ratio of the inertial forces to the viscous forces. It could also be considered the ratio of the total momentum transfer to the molecular momentum transfer.

While there is no theorem relating the non-dimensional Reynolds number (Re) to turbulence, flows at Reynolds number larger than 5000 are typically (but not necessarily) turbulent, while those at low Reynolds number usually remain laminar.

1.2.6(d) Schmidt Number

The Schmidt number Sc is a dimensionless number defined as the ratio of momentum diffusivity and mass diffusivity, and used to characterize fluid flows in which the momentum and mass diffusion convection processes happen simultaneously (Incropera and De Witt, 1990). Mathematically, it is defined as

$$\mathrm{Sc} = \frac{\text{viscous diffusion rate}}{\text{molecular (mass) diffusion rate}} = \frac{\nu}{D} = \frac{\mu}{\rho D},$$

where ν is the kinematic viscosity, D is the mass diffusion coefficient, μ is the dynamic viscosity of the fluid, ρ is the density of the fluid. The heat transfer analog of the Schmidt number is the Prandtl number.

1.2.6(e) Péclet Number

The Péclet number Pe is a dimensionless number represents the ratio of the rate of advection of a physical quantity by the flow to the rate of diffusion of the same quantity driven by an appropriate gradient (Patankar, 1980). The Péclet number defined as

$$\mathrm{Pe} = \frac{\text{advective transport rate}}{\text{diffusive transport rate}}.$$

For diffusion of heat (mass diffusion), it is defined as

$$\mathrm{Pe} = \frac{LU}{D} = \mathrm{Re}_L/\mathrm{Sc}.$$

For diffusion of heat (thermal diffusion), the Péclet number is defined as

$$\mathrm{Pe} = \frac{LU}{\alpha} = \mathrm{Re}/L\mathrm{Pr},$$

where L is the characteristic length, U is the velocity, D is the mass diffusion coefficient, α is the thermal diffusivity, Re_L is the Reynolds number based on the characteristic length and Sc is the Schmidt number. For heat transfer, the Péclet number is the product of the Reynolds number and Prandtl number.

1.2.6(f) Biot Number

The Biot number Bi is a dimensionless quantity defined as the ratio of the heat transfer resistances inside of and at the surface of a body (Incropera et al., 2007). The Biot number can be written as

$$\mathrm{Bi} = \frac{\text{conductive resistance in solid}}{\text{convective resistance in thermal boundary layer}} = \frac{h L_c}{\kappa_b},$$

where h is the heat transfer coefficients, L_c is the characteristic length, which is oftenly defined as the volume of the body divided by the surface area of the body, such that $L_c = \dfrac{V_{\text{body}}}{A_{\text{surface}}}$ and κ_b is the thermal conductivity of the body.

1.2.6(g) Grashof Number

The Grashof number Gr is the ratio of the buoyancy force resulting from temperature to viscous force acting on a fluid (Incropera and Dewitt, 1996; Cengel, 2007). It frequently arises in the study involving natural convection. It represents the thermal buoyancy effect and defines as

$$\mathrm{Gr} = \frac{\text{buoyancy force}}{\text{viscous force}} = \frac{g\beta\,(T_s - T_\infty)\,L^3}{\nu^2},$$

where g is the gravitational acceleration, β is the volumetric thermal expansion coefficient, T_s is the surface temperature, T_∞ is the temperature of the fluid sufficiently far from the surface, L is the characteristic length and ν is the kinematic viscosity of the fluid.

The boundary layer is turbulent at higher Grashof number and laminar at lower Grashof number.

1.2.6(h) Lewis Number

The Lewis number Le is the ratio of thermal diffusivity to mass diffusivity (Klinkenberg and Mooy, 1948). It is used to characterize fluid flows when there is simultaneous heat and mass transfer by convection. Mathematically, the Lewis number can be defined as

$$\text{Le} = \frac{\text{thermal diffusivity}}{\text{mass diffusivity}} = \frac{\alpha}{D},$$

where α is the thermal diffusivity and D is the mass diffusivity. It can also be expressed in terms of the Schmidt number and the Prandtl number,

$$\text{Le} = \frac{\text{Sc}}{\text{Pr}}.$$

1.2.6(i) Skin Friction Coefficient

The skin friction coefficient C_f is a dimensionless shear stress on the surface of a body due to fluid motion (White, 2011) and defined by

$$C_f = \frac{\tau_w}{\frac{1}{2}\rho U_\infty^2},$$

where τ_w is the local shearing stress on the surface of the body, U_∞ is the free stream velocity and ρ is the fluid density.

The skin friction coefficient is also important for practical problems because it determines the heating of the body due to shear stress on the body and heat loss by friction. From the mathematical point of view, (or theoretically) this coefficient is important, to determine the nature of the flow and its separation (when the skin friction equals zero) from the body surface. When the flow separates from the body, it becomes unstable and rotational. The phenomenon of separation is very important for designing and building of a plane. In short, there are many such kinds of practical situations where the skin friction coefficient plays a fundamental importance.

1.2.7 Similarity Solutions

A similarity solution is one in which the number of independent variables is reduced by at least one, usually by a coordinate transformation. The purpose of the similarity transformations is to reduce the set of partial differential equations to ordinary differential equations with pertinent initial and boundary conditions. The idea of transforming the boundary layer equations to another set of equations amiable to known techniques, led to an interesting class of solutions called the similar solutions. Here, the definition of the similar solutions as those for which the component u of the velocity has the property that two velocity profiles $u(x,y)$ are located at different coordinates of x and differ only by a scale factor in u and y. Therefore, if the velocity profiles $u(x,y)$ are plotted in coordinates which have been made dimensionless with reference to the scale factors, then, the velocity profiles $u(x,y)$ can be made congruent at all values of x. Such velocity profiles will also sometimes be called affine. The scale factor for u is denoted by $U(x)$ because from zero to unity, the dimensionless $u(x)$ varies with y at all sections and $U(x)$ is the local potential velocity. The $g(x)$ must be